[*Article*]

Chiral and Achiral Pendant-Bound Poly(biphenylylacetylene)s Bearing Amide and/or Carbamate Groups: One-Handed Helix Formations and Chiral Recognition Abilities

Tomoyuki Ikai,[†,‡,] Shogo Okuda,[†] Motoki Aizawa,[†] Eiji Yashima[†,]**

[†] Department of Molecular and Macromolecular Chemistry, Graduate School of Engineering, Nagoya University, Chikusa-ku, Nagoya 464-8603, Japan

[‡] Precursory Research for Embryonic Science and Technology (PRESTO), Japan Science and Technology Agency (JST), Kawaguchi, Saitama 332-0012, Japan

* Correspondence: ikai@chembio.nagoya-u.ac.jp; yashima@chembio.nagoya-u.ac.jp

ABSTRACT

A series of *cis*-poly(biphenylylacetylene) (PBPA) derivatives bearing chiral and achiral pendant groups at the 4'-position of the biphenyl units through an amide (–NHCO–) or carbamate (–NHCOO–) linker were synthesized by polymerization of the corresponding biphenylylacetylene (BPA) monomers that can be readily prepared in one step from a novel amino-functionalized BPA. An excess one-handed helix induction in the PBPAs through covalent and noncovalent chiral interactions and their chiral recognition abilities when used as chiral stationary phases (CSPs) for high-performance liquid chromatography (HPLC) were investigated. PBPAs bearing optically-pure L-amino acid residues showed unique two-state helical conformational changes between the extended and contracted helices regulated by the solvent-mediated on/off switching of the intramolecular hydrogen-bonding formations between the pendants or at each pendant. The chiral recognition abilities of the helical PBPAs were significantly influenced by the kinds of the pendant L-amino acid residues. The preferred-handed contracted helical PBPA carrying an L-leucine derived pendant showed an excellent chiral resolving power toward various racemic compounds including axially and point chiral compounds and chiral metal complexes. The elution orders of some racemates were completely reversed when its helical conformation was changed to the extended helix. On the other hand, the *trans*-enriched nonhelical L-leucine-bound PBPA derived from its preferred-handed *cis*-helical PBPA and achiral pendant-bound *cis*-helical PBPAs induced by noncovalent chiral interactions and subsequent static memory of the helicity showed a poor and no chiral recognition, respectively.

INTRODUCTION

The synthesis of novel helical polymers with a one-handed helical conformation has been one of the attractive research topics[1-13] because of the potential for their practical applications to high-performance chiral materials as chiral stationary phases (CSPs) for chromatographic enantioseparation,[14-17] asymmetric catalysts,[18-21] and enantioselective sensing devices.[22-24]

We previously reported a series of dynamically-racemic helical poly(biphenylylacetylene)s (PBPAs) bearing methoxymethoxy (MOM) groups at the 2,2'-positions along with various substituents at the 4'-position of the biphenyl pendants,[25] such as achiral[26,27] or chiral[28] aliphatic (e.g., poly-**A**–poly-**D** in Figure 1a), aromatic,[29,30] and oligo(ethylene glycol) groups,[31] through ether (–O–),[26,27,29] ester (–COO– and –OCO–),[27,28,30,31] and carbamate (–OCONH–)[27] linkers. The PBPAs are inherently optically-inactive, but excess one-handed helical and twisted conformations are induced in the polymer backbones and biphenyl pendants in a synchronized manner, respectively, through noncovalent interactions with chiral inducers, such as (*R*)- and (*S*)-1-phenylethanol ((*R*)- and (*S*)-PEA).[25-31] The main-chain helicity and biphenyl axial chirality induced in the PBPAs can be completely retained ("*memorized*") after removal of the chiral inducers.[25-31] The functional substituents introduced at the 4'-position of the biphenyl units significantly affected the helicity induction kinetics, helical sense preference, and stability of the static helicity memory.[25,27,30]

Taking advantage of this exclusively unique static helicity memory observed in the PBPAs, we have developed the first switchable CSPs,[26,27] which enable the elution orders of the enantiomers to be reversibly switched during high-performance liquid chromatography (HPLC) enantioseparation as well as highly-sensitive chirality sensors,[32,33] switchable asymmetric catalysts,[29,34] and circularly polarized luminescent materials.[31] In addition, when a small amount

of the chiral substituents was introduced at the 4'-position of the chiral/achiral copolymers of the PBPAs, one-handed helical PBPAs could be readily produced through the hierarchical chirality transfer from the covalently-linked chiral substituents to the axially-chiral biphenyl units and further to the polymer backbones due to a remarkably strong amplification of the asymmetry.[31,35,36]

In this study, we designed and synthesized a new series of dynamically-racemic helical (poly-**1**$^{\mathbf{Am}}$, poly-**1**$^{\mathbf{Car}}$, and poly-**2**$^{\mathbf{Gly}}$) and excess one-handed helical (poly-**2**$^{\mathbf{L\text{-}Ala}}$, poly-**2**$^{\mathbf{L\text{-}Leu}}$, poly-**2**$^{\mathbf{L\text{-}Ile}}$, and poly-**2**$^{\mathbf{L\text{-}Phe}}$) PBPAs bearing achiral and L-amino acid residues at the 4'-position of the biphenyl units, respectively, through an amide (–NHCO–) linker except for poly-**1**$^{\mathbf{Car}}$ carrying a carbamate (–NHCOO–) linkage; the sequence is opposite to that of the previously reported poly-**D** (–OCONH–)[27] (Figure 1b,c). The preferred-handed helix forming capabilities of the dynamically-racemic helical PBPAs using (*R*)-and (*S*)-PEA as a helix inducer followed by static helicity memory behaviors (Figure 1b), the effect of the L-amino acid residues on an excess one-handed helix formation of the PBPAs in different solvents (Figure 1c), and their chiral recognition abilities as CSPs for HPLC were investigated.

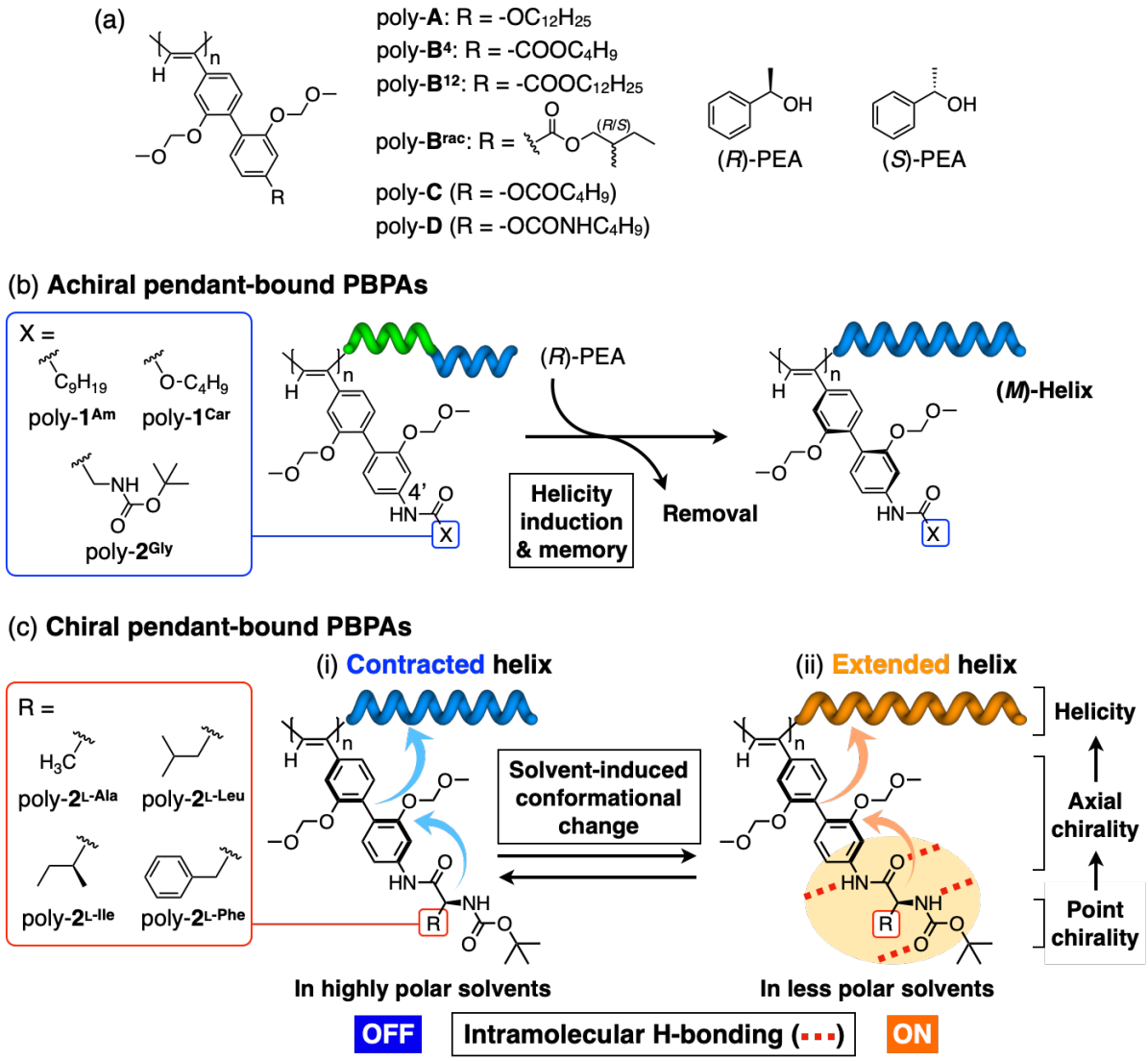

Figure 1. (a) Structures of PBPAs (poly-**A** – poly-**D**) and optically-active 1-phenylethanol ((*R*)- and (*S*)-PEA). (b) Schematic illustration of macromolecular helicity induction and subsequent helicity memory in achiral pendant-bound PBPAs (poly-$\mathbf{1}^{\mathbf{Am}}$, poly-$\mathbf{1}^{\mathbf{Car}}$ and poly-$\mathbf{2}^{\mathbf{Gly}}$) through noncovalent chiral interactions with optically active alcohol ((*R*)-PEA). (c) Schematic illustration of the solvent-induced conformational changes of L-amino acid pendant-bound PBPAs (poly-$\mathbf{2}^{\mathbf{L\text{-}Ala}}$, poly-$\mathbf{2}^{\mathbf{L\text{-}Leu}}$, poly-$\mathbf{2}^{\mathbf{L\text{-}Ile}}$, and poly-$\mathbf{2}^{\mathbf{L\text{-}Phe}}$) between contracted (i) and extended (ii) helices in highly and less polar solvents through off and on switching of intramolecular hydrogen-bonding formations, respectively.

RESULTS AND DISCUSSION

Synthesis.

A novel biphenylylacetylene (BPA) monomer (BPA^{NH2}) with an amino group at the 4'-position of the biphenyl unit was newly synthesized as a key monomer precursor and converted into three achiral (**1**^{Am}, **1**^{Car}, and **2**^{Gly}) and four chiral (**2**$^{L\text{-}Ala}$, **2**$^{L\text{-}Leu}$, **2**$^{L\text{-}Ile}$, and **2**$^{L\text{-}Phe}$) monomers carrying amide (–NHCO–) and/or carbamate (–NHCOO–) functional groups at the 4'-position of the biphenyl unit (Scheme S1). The achiral monomers **1**^{Am} and **1**^{Car} were then polymerized with a rhodium catalyst ($[Rh(nbd)Cl]_2$, nbd: norbornadiene) in tetrahydrofuran (THF) in the presence of triethylamine at 30 °C according to a previously reported method (Scheme S2),[26-30] producing *cis-transoidal* poly-**1**^{Am} and poly-**1**^{Car} in high yields (≥97%) (Figure S1 and Table 1).[37,38] Achiral- (**2**^{Gly}) and L-amino acid pendant-bound (**2**$^{L\text{-}Ala}$, **2**$^{L\text{-}Leu}$, **2**$^{L\text{-}Ile}$, and **2**$^{L\text{-}Phe}$) BPAs were polymerized using a multicomponent catalytic system with $[Rh(nbd)Cl]_2$ as a catalyst in THF/*N*,*N*-dimethylformamide (DMF) (4/1, v/v) at 30 °C,[39] almost quantitatively yielding the *cis-transoidal* PBPAs (Scheme S3 and Table 2).[40] The number-average molar masses (M_n) of the polymers were estimated to be more than 1.7×10^5 by size-exclusion chromatography (SEC) (Tables 1 and 2).

Table 1. Polymerization Results of 1^{Am} and 1^{Car} with $[Rh(nbd)Cl]_2$ in THF/Et_3N at 30 °C for 3 h [a]

entry	monomer	polymer			
		sample code	yield (%)[b]	M_n (10^5)[c]	M_w/M_n [c]
1	$\mathbf{1}^{Am}$	poly-$\mathbf{1}^{Am}$	98	12.3	1.41
2	$\mathbf{1}^{Car}$	poly-$\mathbf{1}^{Car}$	97	6.34	1.97

[a] [Monomer] = 0.23 M, $[[Rh(nbd)Cl]_2]$ = 1.3 mM. [b] *n*-Hexane insoluble part. [c] Determined by SEC (polystyrene standards) with DMF containing 0.5 wt% tetra-*n*-butylammonium bromide (TBAB) as the eluent.

Table 2. Polymerization Results of 2^{Gly}, $2^{L\text{-}Ala}$, $2^{L\text{-}Leu}$, $2^{L\text{-}Ile}$, and $2^{L\text{-}Phe}$ with $[Rh(nbd)Cl]_2$ in the Presence of 4-Propoxyphenylboronic Acid, Diphenylacetylene, PPh_3, and KOH in THF/DMF at 30 °C for 3 h [a]

		polymer			
entry	monomer	sample code	yield (%)[b]	M_n (10^5)[c]	M_w/M_n [c]
1	$\mathbf{2}^{Gly}$	poly-$\mathbf{2}^{Gly}$	93	2.03	2.53
2	$\mathbf{2}^{L\text{-}Ala}$	poly-$\mathbf{2}^{L\text{-}Ala}$	96	1.73	1.53
3	$\mathbf{2}^{L\text{-}Leu}$	poly-$\mathbf{2}^{L\text{-}Leu}$	97	2.03	1.26
4	$\mathbf{2}^{L\text{-}Ile}$	poly-$\mathbf{2}^{L\text{-}Ile}$	98	2.03	1.59
5	$\mathbf{2}^{L\text{-}Phe}$	poly-$\mathbf{2}^{L\text{-}Phe}$	92	2.15	1.62

[a] [Monomer] = 0.5 M, $[[Rh(nbd)Cl]_2]$ = 1.25 mM, $[[Rh(nbd)Cl]_2]$/[4-propoxyphenylboronic acid]/[diphenylacetylene]/$[PPh_3]$/[KOH] = 1/3/8/6/5. [b] *n*-Hexane insoluble part. [c] Determined by SEC (polystyrene standards) with DMF containing 0.5 wt% TBAB as the eluent.

Macromolecular Helicity Induction and Static Helicity Memory of Achiral Pendant-Bound PBPAs.

The poly-**1**$^{\mathbf{Am}}$, poly-**1**$^{\mathbf{Car}}$, and poly-**2**$^{\mathbf{Gly}}$ composed of achiral monomer units displayed intense circular dichroisms (CDs) induced by (*R*)-PEA in THF (20 vol%) at 25 °C in the polymer backbone chromophore regions (Figure 2(i)). The split-type induced Cotton effect patterns were similar to each other, but their Cotton effect signs were opposite to those of the previously reported right (*P*)-handed helical PBPAs (poly-**A** – poly-**D**) induced by (*R*)-PEA,[26-28] indicating that an opposite (*M*)-handed helix was induced in the present achiral pendant-bound PBPAs.[41] The reason is not clear at present, but the amide (–NHCO–) and carbamate (–NHCOO–) functional groups newly introduced at the 4'-position of the biphenyl units of the PBPAs most likely contributed to the observed opposite helix formation. The induced CD (ICD) intensities of poly-**1**$^{\mathbf{Am}}$ and poly-**1**$^{\mathbf{Car}}$ rapidly reached almost plateau values within 1 and ca. 5 min at 25 °C, respectively, as observed for poly-**A**,[27] but gradually increased with time at –10 °C, reaching almost the same values at 25 °C after ca. 24 h (Figure S2a,b(i,ii)). In contrast, a much longer time was required for poly-**2**$^{\mathbf{Gly}}$ to induce a preferred-handed helix even showing a weaker CD at 25 and –10 °C (Figure S2a,b(iii)). Thus, the one-handed helix forming rate increased in the following order: poly-**2**$^{\mathbf{Gly}}$ << poly-**1**$^{\mathbf{Car}}$ < poly-**1**$^{\mathbf{Am}}$. The ICD intensities of the polymers slightly increased at −10 °C in THF/(*R*)-PEA (8/2, v/v) (Figure 2(ii)). When (*S*)-PEA (20 vol %) was used as a helix inducer, the enantiomeric right (*P*)-handed helices were induced in the polymers, resulting in the mirror image ICDs (Figure 2(iv)). The CD titration experiments demonstrated that the ICD intensities of poly-**1**$^{\mathbf{Am}}$ and poly-**1**$^{\mathbf{Car}}$ reached nearly saturated second Cotton effects ($\Delta\varepsilon_{2nd}$ = 16.3 and 16.1, respectively) in the presence of 50 vol% of (*R*)-PEA in THF, in which the helix-sense excess (*hse*) values were estimated to be 82 and 81%, respectively (Figure S3).[42] On the other hand, the $\Delta\varepsilon_{2nd}$ value of poly-**2**$^{\mathbf{Gly}}$

monotonically increased with an increase in the (*R*)-PEA content in THF, and its maximum *hse* value reached 72% ($\Delta\varepsilon_{2nd}$ = 14.3) even in pure (*R*)-PEA, which was lower than those of poly-**1**$^{\mathbf{Am}}$ (82% *hse*) and poly-**1**$^{\mathbf{Car}}$ (81% *hse*) in THF/(*R*)-PEA (5/5, v/v). The observed slow and insufficient helix induction in poly-**2**$^{\mathbf{Gly}}$ with (*R*)-PEA (Figures 2, S2, and S3) compared to those of poly-**1**$^{\mathbf{Am}}$ and poly-**1**$^{\mathbf{Car}}$ were probably due to the polar carbamate group located away from the biphenyl unit that would prevent attractive noncovalent chiral interactions between the biphenyl units and (*R*)-PEA.

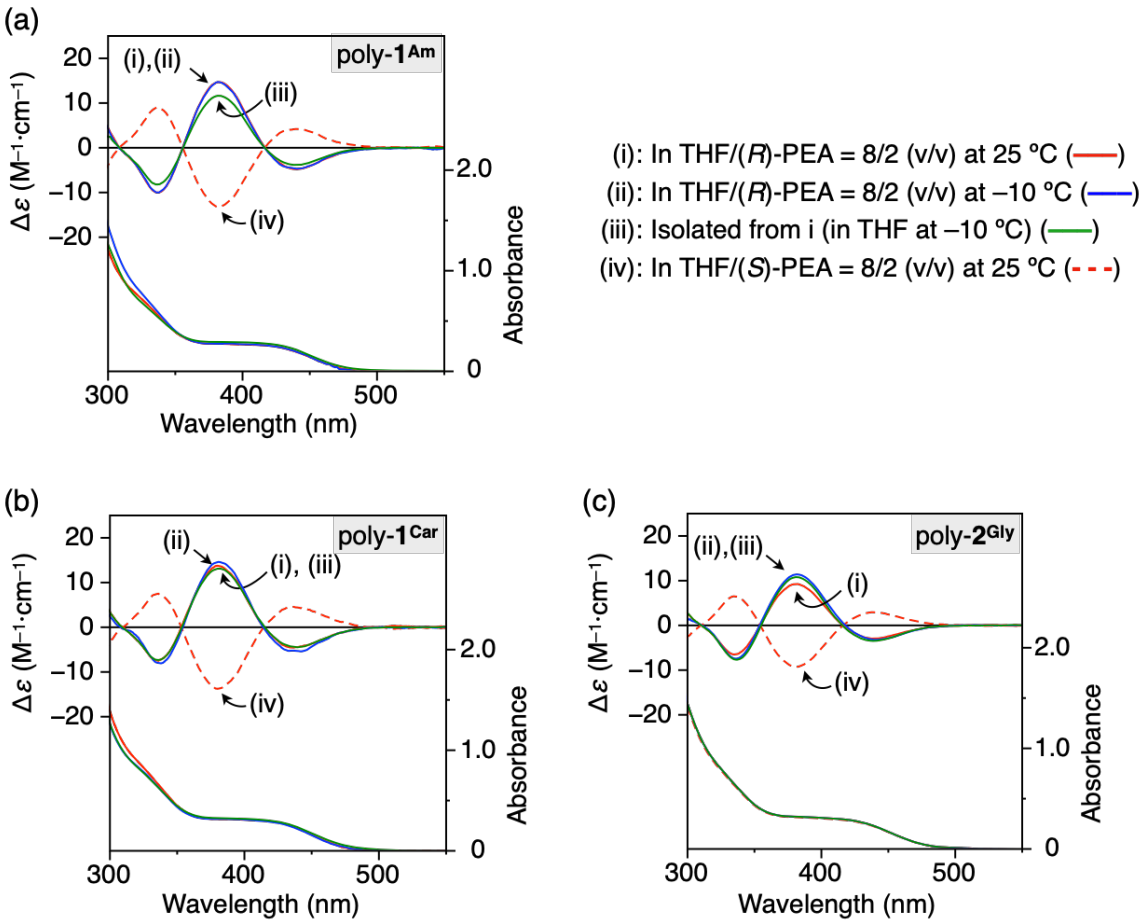

Figure 2. CD and absorption spectra of poly-**1**$^{\mathbf{Am}}$ (a), poly-**1**$^{\mathbf{Car}}$ (b), and poly-**2**$^{\mathbf{Gly}}$ (c) in the presence of (*R*)-PEA (i,ii) and (*S*)-PEA (iv) in THF (THF/PEA = 8/2, v/v) measured at 25 (i,iv) and –10 (ii) °C after storage at 25 °C for 12 h, and the isolated polymers recovered from ii (iii), measured in THF at –10 °C. [Monomer units of polymer] = 1.0 mM.

The preferred-handed helical conformations of poly-**1**$^{\mathbf{Am}}$, poly-**1**$^{\mathbf{Car}}$, and poly-**2**$^{\mathbf{Gly}}$ biased by (*R*)-PEA were efficiently memorized in THF after complete removal of (*R*)-PEA (Figures 2(iii), S4, and S5), resulting in the helicity-memorized (*M*)-*h*-poly-**1**$^{\mathbf{Am}}$, (*M*)-*h*-poly-**1**$^{\mathbf{Car}}$, and (*M*)-*h*-poly-**2**$^{\mathbf{Gly}}$, respectively. The ICD intensities derived from the static helicity memory gradually decreased with time in THF at –10 °C and their half-life time periods ($t_{1/2}$) were roughly estimated to be 4–5 h (Figure S6). Because the $t_{1/2}$ value of the previously reported poly-**B**$^{\mathbf{12}}$ bearing ester groups (-COO-) at the 4'-position of the biphenyl units was more than 3 days under the same conditions,[27] the introduction of the amide (–NHCO–) or carbamate (–NHCOO–) linkage at the 4'-position of the biphenyl units likely destabilized the static helicity memories of the helical PBPAs.

Chiral Recognition Abilities of Helicity-Memorized PBPA-Based CSPs for HPLC.

The novel helicity-memorized PBPA-based CSPs consisting of (*M*)-*h*-poly-**1**$^{\mathbf{Am}}$, (*M*)-*h*-poly-**1**$^{\mathbf{Car}}$, and (*M*)-*h*-poly-**2**$^{\mathbf{Gly}}$ were then prepared according to a previously reported method[27,28,30] by coating each polymer solution in THF/(*R*)-PEA (8/2, v/v), showing the maximum ICD signals, on macroporous silica gel, followed by evaporating THF and complete removal of (*R*)-PEA by washing with *n*-hexane before packing into a stainless-steed column (for details of the preparation of the CSPs for HPLC, see section 5 in the Supporting Information (SI)). The static helicity memories of (*M*)-*h*-poly-**1**$^{\mathbf{Am}}$, (*M*)-*h*-poly-**1**$^{\mathbf{Car}}$, and (*M*)-*h*-poly-**2**$^{\mathbf{Gly}}$ coated on silica gel were not stable as anticipated, as confirmed by the CD measurements of the polymers recovered from the CSPs in THF at –10 °C; the CD intensities were reduced to 20, 60, and 78% of those before coating on silica gel, respectively (Figure S7). Because of the significant loss of the helicity memory of poly-**1**$^{\mathbf{Am}}$ during the coating process, we investigated the chiral recognition abilities of (*M*)-*h*-poly-**1**$^{\mathbf{Car}}$- and (*M*)-*h*-poly-**2**$^{\mathbf{Gly}}$-based CSPs using *n*-hexane–2-propanol (97/3, v/v) as the eluent at –

10 °C. Unexpectedly, these CSPs could not resolve all the tested racemates (**3**–**11**; see Figure 4a) (Table S1), despite the facts that some racemates were almost completely separated into enantiomers on helical PBPAs with static helicity memory carrying functional ester (-COO- (poly-**B**^{4} and poly-**B**^{rac}) and -OCO- (poly-**C**))[27,28] and carbamate linkages (-OCONH- (poly-**D**))[27] at the 4'-position of the biphenyl units; the linkage sequence of poly-**D** is opposite to that of poly-**1**^{Car} (–NHCOO–). These results suggest that the –NHCOO– and –NHCO– linkages introduced at the 4'-position of the biphenyl units bearing achiral pendants in poly-**1**^{Car} and poly-**2**^{Gly}, respectively, are not suitable as recognition sites for efficient enantioseparation, causing no chiral recognition ability, although the substantial reason for this is still unclear presently because some of the corresponding L-amino acid pendant-bound PBPAs showed high chiral resolving abilities (see below).

Chiroptical Properties of L-Amino Acid Pendant-Bound PBPAs.

We next investigated an excess one-handedness helix formation of the L-amino acid pendant-bound PBPAs in different solvents, such as THF, chloroform, and DMF (Figure 1c). Interestingly, the L-amino acid pendant-bound PBPAs showed unique solvent-induced two-state helical conformational changes (Figure 3). In chloroform and THF at 25 °C, all the L-alanine-bound PBPAs, except for poly-**2**$^{L\text{-}Ala}$ in THF, showed CD spectra quite different from those of (*M*)-*h*-poly-**1**^{Am}, -poly-**1**^{Car}, and -poly-**2**^{Gly} in THF (Figure 2(iii)) and those of the previously reported preferred-handed helical PBPAs (poly-**A** – poly-**D**) in their patterns, accompanied by a large red-shift in the absorption spectra (Figure 3a–d(i,ii)), suggesting an extended helix formation.[22,29,43-46] In polar DMF, however, their CD spectral patterns changed to typical split-type CDs (Figure 3a–d(iii)) similar to those of the (*M*)-handed helical PBPAs including poly-**A** – poly-**D**[26-28] with a

static helicity memory (see Figure 2(iii)).[47] The CD spectral patterns and intensities of poly-**2**$^{\text{L-Leu}}$ in chloroform, THF, and DMF were totally independent of the time, concentrations (0.10–10 mM) (Figure S8), and temperatures (–10 – 50 °C) (Figure S9). Hence, intermolecular aggregate formations can be ruled out for the observed unusual solvent-dependent absorption and CD spectral changes, which are supposed to result from the solvent-induced helical conformational changes of the L-amino acid pendant-bound helical PBPAs that are stable at high temperatures.

To gain insight into the origin of the solvent-induced helical conformational changes, we measured the IR spectra of poly-**2**$^{\text{L-Ala}}$ and poly-**2**$^{\text{L-Leu}}$ in chloroform, THF, and THF/dimethyl sulfoxide (DMSO) (8/2, v/v) with different polarities (Figure S10a,b), in which the polymers showed different CD and absorption spectra (Figures 3a,b and S10c,d). The carbonyl stretching bands of the amide and carbamate groups of poly-**2**$^{\text{L-Leu}}$ in chloroform and THF appeared at ca. 1670 cm^{-1} (Figure S10b(i,ii)), which shifted to higher wavenumbers in THF/DMSO (8/2, v/v) (Figure S10b(iii)). These IR measurement results indicated an intramolecular H-bonding formation of poly-**2**$^{\text{L-Leu}}$ between the neighboring amide and/or carbamate pendant groups along the polymer backbone in chloroform and THF (Figures 1c(ii) and S10), as supported by its extended (*M*)-handed helical model structure (Figure S11a), in which the pendant amide and carbamate residues form intramolecular H-bonding networks along the polymer backbone.[48] In the presence of polar DMSO (20 vol%) in THF as well as in DMF and THF/DMF (8/2, v/v), such intramolecular and/or intrapendant H-bonding formations appear to be hampered or switched off, so that contracted helices similar to those of the previously reported helical PBPAs with no H-bond forming functional groups at the pendants[26-28] are favorably formed as shown in Figure S11b, in which such intramolecular H-bonds could not be formed, thus showing typical CD and absorption spectra as observed in other L-amino acid pendant-bound PBPAs (Figures 1c(i), 3a–

d(iii), S10c,d(iii), and S12a–d(i)). The solvent-dependent CD/absorption and IR spectral changes in poly-**2**$^{\text{L-Ala}}$ showed a similar tendency except for those in THF (Figure S10a,c).

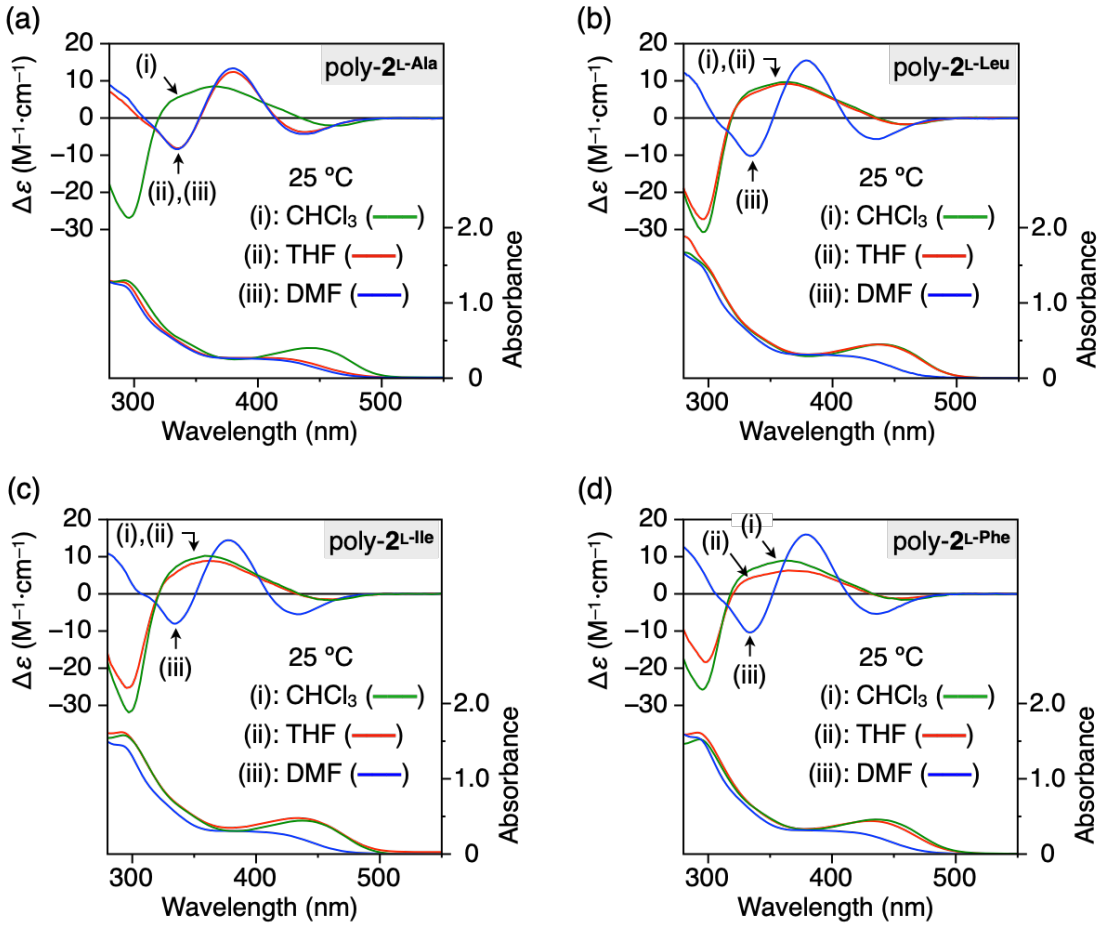

Figure 3. CD and absorption spectra of poly-**2**$^{\text{L-Ala}}$ (a), poly-**2**$^{\text{L-Leu}}$ (b), poly-**2**$^{\text{L-Ile}}$ (c), and poly-**2**$^{\text{L-Phe}}$ (d) in chloroform (i), THF (ii), and DMF (iii) measured at 25 °C after storage at 25 °C for 30 min. [Monomer units of polymer] = 1.0 mM.

Chiral Recognition Abilities of L-Amino Acid Pendant-Bound PBPA-based CSPs for HPLC

We anticipated that the observed solvent-induced two-state helical conformational changes in the L-amino acid pendant-bound PBPAs would provide unique CSPs for HPLC, showing different resolution abilities by changing the coating solvents on silica gel. To this end, extended and contracted helical poly-**2**$^{\text{L-Leu}}$-based CSPs were first prepared using THF and THF/DMF (8/2, v/v) as the coating solvents, respectively (for details, see section 5 in the SI). The HPLC enantioseparation results of nine racemates (**3**–**11**) monitored with dual UV and CD detectors were evaluated based on the retention ($k_1 = (t_1 - t_0)/ t_0$) and separation ($\alpha = (t_2 - t_0)/ (t_1 - t_0)$) factors (see Figure 4b(i)) and the results are summarized in Table 3, where t_1 and t_2 are the retention times of the first- and second-eluted enantiomers, respectively, and t_0 is the hold-up time.

In sharp contrast to the (*M*)-*h*-poly-**1**$^{\text{Car}}$- and (*M*)-*h*-poly-**2**$^{\text{Gly}}$-based CSPs, both the contracted and extended helical poly-**2**$^{\text{L-Leu}}$s, in particular, the contracted helical poly-**2**$^{\text{L-Leu}}$ showed excellent chiral recognition abilities and resolved all the nine racemates including the axially (**3** and **4**) and point (**5** and **9**–**11**) chiral compounds and chiral metal acetylacetonate complexes (**6**–**8**) with the α values of more than 2 for **6** and **8** (Table 3), as demonstrated in the typical chromatograms for the base-line separation of the **3**, **8**, and **11** enantiomers (Figure 4b and c(iv)). The helical conformation of the contracted helical poly-**2**$^{\text{L-Leu}}$ coated on silica gel almost remained unchanged as confirmed by its CD spectrum recovered from the CSP (Figure S13). It is noteworthy that the *trans*-enriched nonhelical poly-**2**$^{\text{L-Leu}}$ derived from its *cis*-helical poly-**2**$^{\text{L-Leu}}$ by grinding,[34,49,50] which completely lost its CD induced in the polymer backbone (Figure S14), showed a poor resolving ability when used as a CSP (Table 3). The elution order of **7** on the nonhelical poly-**2**$^{\text{L-Leu}}$ was opposite to that on the contracted (*M*)-helical *cis*-poly-**2**$^{\text{L-Leu}}$, indicating the dominant role of the macromolecular helicity over the pendant L-leucine residues in chiral recognition.

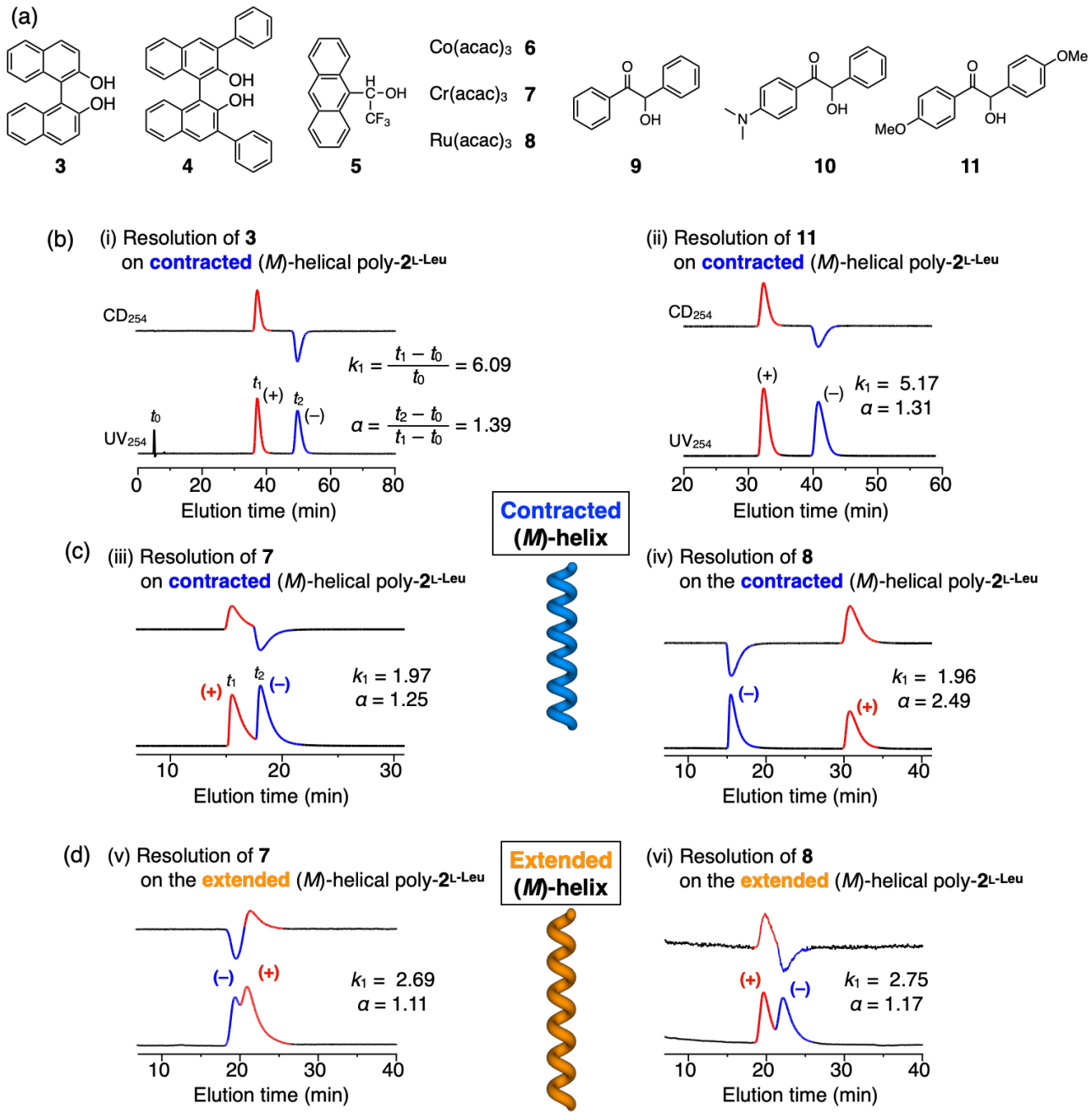

Figure 4. (a) Structures of racemates (**3**–**11**). (b–d) HPLC chromatograms for the resolutions of **3** (i), **11** (ii), **7** (iii,v) and **8** (iv,vi) on the contracted (b,c) and extended (d) (*M*)-handed helical poly-**2**$^{\text{L-Leu}}$-based CSPs under normal-phase conditions at –10 °C. Eluent: *n*-hexane/2-propanol (97/3, v/v).

Table 3. Resolution Results of Racemates 3–11 on (*M*)-Handed Helical Poly-2$^{L\text{-Ala}}$, -Poly-2$^{L\text{-Leu}}$, -Poly-2$^{L\text{-Ile}}$, and -Poly-2$^{L\text{-Phe}}$-Based CSPs at –10 °C [a]

		contracted helical (*M*)-poly-**2**$^{L\text{-Ala}}$		contracted helical (*M*)-poly-**2**$^{L\text{-Leu}}$		extended helical (*M*)-poly-**2**$^{L\text{-Leu}}$		*trans*-enriched nonhelical poly-**2**$^{L\text{-Leu}}$		contracted helical (*M*)-poly-**2**$^{L\text{-Ile}}$		contracted helical (*M*)-poly-**2**$^{L\text{-Phe}}$	
		THF/DMF [b] (8/2, v/v)		THF/DMF [b] (8/2, v/v)		THF [b]		THF/DMF [b] (8/2, v/v)		THF/DMF [b] (8/2, v/v)		THF/DMF [b] (8/2, v/v)	
run	racemate	k_1	α	k_1	α	k_1	α	k_1	α	k_1	α	k_1	α
1	**3**	– [c]	– [c]	6.09	1.39 (+)	6.09	ca.1 (+)	2.31	ca.1 (+)	6.56	1.04 (+)	– [c]	– [c]
2	**4**	6.18	ca.1 (+)	2.15	1.38 (+)	2.57	1.11 (–)	2.15	ca.1 (+)	2.41	ca.1 (+)	– [c]	– [c]
3	**5**	1.71	1.0	1.45	1.16	1.61	1.0	1.71	1.0	1.61	1.0	1.79	1.0
4	**6**	1.27	1.26 (+)	1.42	2.03 (–)	2.23	1.16 (+)	1.92	1.12 (–)	0.86	1.71 (+)	1.99	1.19 (+)
5	**7**	1.76	1.40 (–)	1.97	1.25 (+)	2.69	1.11 (–)	2.01	1.11 (–)	1.07	1.27 (–)	2.43	1.22 (–)
6	**8**	2.09	ca.1 (+)	1.96	2.49 (–)	2.75	1.17 (+)	1.20	1.20 (–)	0.94	1.93 (+)	3.34	ca.1 (+)
7	**9**	1.81	1.0	1.40	1.20 (–)	1.38	1.14 (–)	1.49	ca.1 (–)	1.41	1.14 (–)	2.40	1.0
8	**10**	5.85	1.0	4.45	1.05 (+)	– [c]	– [c]	4.55	ca.1 (+)	4.17	1.24 (+)	8.70	1.0
9	**11**	7.45	1.0	5.17	1.31 (+)	– [c]	– [c]	6.01	ca.1 (+)	5.00	1.26 (+)	11.8	ca.1 (+)

[a] Column: 25 x 0.20 (i.d.) cm; eluent: *n*-hexane–2-propanol (97/3, v/v); flow rate: 0.15 ml/min. The signs in parentheses represent the Cotton effect signs at 254 nm of the first-eluted enantiomers. [b] Coating solvent. [c] Not eluted.

The extended helical poly-**2**$^{\text{L-Leu}}$-based CSP prepared from its THF solution also exhibited a relatively high chiral recognition ability and resolved five racemates (**4** and **6**–**9**) (Table 3). Interestingly, the elution orders of some enantiomers **(4** and **6**–**8**) on the contracted and extended helical poly-**2**$^{\text{L-Leu}}$-based CSPs were reversed from each other (Table 3), as shown in the typical chromatograms for the separation of **7** and **8 (**Figure 4c,d), indicative of developing a switchable CSP which can be possible by treatment with different solvents, resulting from two-state helical conformational changes between the contracted and extended helices. Although a number of solvent-induced helical conformational changes in the synthetic helical polymers has been reported,[7,25] to the best of our knowledge, switching of the elution orders of the enantiomers when applied to CSPs has not been achieved.[51-54]

Considering the better resolution ability of the contracted helical poly-**2**$^{\text{L-Leu}}$ than that of the extended helical counterpart, probably due to the polar amide and carbamate groups free from intramolecular H-bonds, which can function as effective chiral recognition sites, we then investigated the chiral recognition abilities of the contracted helical poly-**2**$^{\text{L-Ala}}$-, poly-**2**$^{\text{L-Ile}}$-, and poly-**2**$^{\text{L-Phe}}$-based CSPs prepared from each polymer solution in THF/DMF (8/2, v/v) (Table 3). Among them, poly-**2**$^{\text{L-Ile}}$ exhibited a high chiral recognition and resolved seven racemates (**3** and **6**–**11**), while the resolving abilities of poly-**2**$^{\text{L-Ala}}$ and poly-**2**$^{\text{L-Phe}}$ were as low as that of the *trans*-enriched nonhelical poly-**2**$^{\text{L-Leu}}$. Hence, the chiral recognition abilities of the L-amino acid pendant-bound contracted helical PBPAs tended to decrease in the following order: poly-**2**$^{\text{L-Leu}}$ > poly-**2**$^{\text{L-Ile}}$ >> poly-**2**$^{\text{L-Ala}}$ ≥ poly-**2**$^{\text{L-Phe}}$. All the L-amino acid pendant-bound contracted helical PBPAs displayed the same split-type ICDs with approximately similar intensities and hence, similar *hse* values (Figure 3). Therefore, the observed remarkable differences in their chiral recognition abilities are mostly ascribed to the substituents of the L-amino acid residues of the PBPAs. Poly-

2$^{\text{L-Leu}}$ and poly-**2**$^{\text{L-Ile}}$ carry modest-sized *iso*- and *sec*-butyl substituents, respectively, which likely contribute to favorably arranging the polar amide and carbamate functional groups at the pendants in an excess one-handed array along the contracted helical backbones, thereby enabling efficient chiral interactions with the racemates in a highly-enantioselective manner, although the elution orders of the **6**–**8** enantiomers were only reversed on the contracted helical poly-**2**$^{\text{L-Leu}}$-based CSP (Table 3).

CONCLUSIONS

We have synthesized a series of new PBPAs bearing achiral and homochiral L-amino acid pendant groups at the 4'-position of the biphenyl units through an amide or carbamate linkage. In the former PBPAs, excess one-handed helices were successfully induced and simultaneously memorized via noncovalent chiral interactions with chiral alcohols, although their chiral recognition abilities when used as CSPs for HPLC were unexpectedly low. By introducing the homochiral L-amino acid residues into the pendants, the PBPAs instantly formed excess (*M*)-handed helices and showed unique solvent-induced two-state helical conformational changes between the extended and contracted helices triggered by on/off switching of the intramolecular H-bonding formations in less polar and polar solvents, respectively, which were independent of the pendant L-amino acid residues. The chiral resolving abilities of the helical PBPAs were, however, significantly affected by the kinds of the pendant L-amino acid residues and their backbone structures (extended or contracted helix). Among the extended and/or contracted helical PBPAs investigated as CSPs, the contracted (*M*)-handed helical PBPA bearing an L-leucine derived pendant showed the highest chiral recognition toward various racemic compounds, while the corresponding extended helical PBPA separated some racemates with a reversed elution order.

The essential role of the one-handed helicity over the pendant L-leucine residues in chiral recognition was unambiguously demonstrated by the fact that the corresponding nonhelical L-leucine-bound PBPA exhibited a poor chiral recognition. We have recently developed a versatile method to produce immobilized-type CSPs, through which helical PBPA chains can be covalently bonded to silica gel.[27] Using this technique, we believe that more powerful PBPA-based switchable CSPs with a high durability against solvents capable of switching the elution orders of a wide variety of enantiomers will be developed by further introducing a particular chiral functional group at the biphenyl units. Work toward these goals is now underway in our laboratory.

ASSOCIATED CONTENT

Supporting Information.

The Supporting Information is available free of charge on the ACS Publications website at DOI: XXX. Full experimental details, characterizations of monomers and polymers, and additional supporting data (PDF).

AUTHOR INFORMATION

Corresponding Author

*ikai@chembio.nagoya-u.ac.jp

*yashima@chembio.nagoya-u.ac.jp

ACKNOWLEDGMENT

We thank Dr. Kosuke Oki (Nagoya University) for molecular modeling. This work was supported in part by JSPS KAKENHI (Grant-in-Aid for Specially Promoted Research, No. 18H05209 (E.Y. and T.I.) and Grant-in-Aid for Scientific Research (B), No. 21H01984 (T.I.)).

REFERENCES

(1) Green, M. M.; Park, J. W.; Sato, T.; Teramoto, A.; Lifson, S.; Selinger, R. L. B.; Selinger, J. V. The Macromolecular Route to Chiral Amplification. *Angew. Chem., Int. Ed.* **1999**, *38*, 3139–3154.

(2) Nakano, T.; Okamoto, Y. Synthetic Helical Polymers: Conformation and Function. *Chem. Rev.* **2001**, *101*, 4013–4038.

(3) Liu, J.; Lam, J. W. Y.; Tang, B. Z. Acetylenic Polymers: Syntheses, Structures, and Functions. *Chem. Rev.* **2009**, *109*, 5799–5867.

(4) Schwartz, E.; Koepf, M.; Kitto, H. J.; Nolte, R. J. M.; Rowan, A. E. Helical Poly(isocyanides): Past, Present and Future. *Polym. Chem.* **2011**, *2*, 33–47.

(5) Fujiki, M. Supramolecular Chirality: Solvent Chirality Transfer in Molecular Chemistry and Polymer Chemistry. *Symmetry* **2014**, *6*, 677–703.

(6) Freire, F.; Quiñoá, E.; Riguera, R. Supramolecular Assemblies from Poly(phenylacetylene)s. *Chem. Rev.* **2016**, *116*, 1242–1271.

(7) Yashima, E.; Ousaka, N.; Taura, D.; Shimomura, K.; Ikai, T.; Maeda, K. Supramolecular Helical Systems: Helical Assemblies of Small Molecules, Foldamers, and Polymers with Chiral Amplification and Their Functions. *Chem. Rev.* **2016**, *116*, 13752–13990.

(8) Liu, L.; Zang, Y.; Jia, H.; Aoki, T.; Kaneko, T.; Hadano, S.; Teraguchi, M.; Miyata, M.; Zhang, G.; Namikoshi, T. Helix-Sense-Selective Polymerization of Achiral Phenylacetylenes and Unique Properties of the Resulting Cis-cisoidal Polymers. *Polym. Rev.* **2017**, *57*, 89–118.

(9) Worch, J. C.; Prydderch, H.; Jimaja, S.; Bexis, P.; Becker, M. L.; Dove, A. P. Stereochemical Enhancement of Polymer Properties. *Nat. Rev. Chem.* **2019**, *3*, 514–535.

(10) Leigh, T.; Fernandez-Trillo, P. Helical Polymers for Biological and Medical Applications. *Nat. Rev. Chem.* **2020**, *4*, 291–310.

(11) Zhang, Y. J.; Deng, J. P. Chiral Helical Polymer Materials Derived from Achiral Monomers and Their Chiral Applications. *Polym. Chem.* **2020**, *11*, 5407–5423.

(12) Percec, V. Merging Macromolecular and Supramolecular Chemistry into Bioinspired Synthesis of Complex Systems. *Isr. J. Chem.* **2020**, *60*, 48–66.

(13) Percec, V.; Xiao, Q. Helical Self-Organizations and Emerging Functions in Architectures, Biological and Synthetic Macromolecules. *Bull. Chem. Soc. Jpn.* **2021**, *94*, 900–928.

(14) Nakano, T. Optically Active Synthetic Polymers as Chiral Stationary Phases in HPLC. *J. Chromatogr. A* **2001**, *906*, 205–225.

(15) Shen, J.; Okamoto, Y. Efficient Separation of Enantiomers Using Stereoregular Chiral Polymers. *Chem. Rev.* **2016**, *116*, 1094–1138.

(16) Zhang, C.; Liu, L.; Okamoto, Y. Enantioseparation Using Helical Polyacetylene Derivatives. *TrAC-Trends Anal. Chem.* **2020**, *123*, 115762.

(17) Wu, G. Recent Advances in Helical Polyacetylene Derivatives Used as Coated Chiral Stationary Phases for Enantioseparation. *Polym. Chem.* **2022**, *13*, 3036–3047.

(18) Megens, R. P.; Roelfes, G. Asymmetric Catalysis with Helical Polymers. *Chem. - Eur. J.* **2011**, *17*, 8514–8523.

(19) Suginome, M.; Yamamoto, T.; Nagata, Y.; Yamada, T.; Akai, Y. Catalytic Asymmetric Synthesis Using Chirality-Switchable Helical Polymer as a Chiral Ligand. *Pure Appl. Chem.* **2012**, *84*, 1759–1769.

(20) Li, Y.; Bouteiller, L.; Raynal, M. Catalysts Supported by Homochiral Molecular Helices: A New Concept to Implement Asymmetric Amplification in Catalytic Science. *ChemCatChem* **2019**, *11*, 5212–5226.

(21) Liu, N.; Zhou, L.; Wu, Z.-Q. Alkyne-Palladium(II)-Catalyzed Living Polymerization of Isocyanides: An Exploration of Diverse Structures and Functions. *Acc. Chem. Res.* **2021**, *54*, 3953–3967.

(22) Maeda, K.; Mochizuki, H.; Watanabe, M.; Yashima, E. Switching of Macromolecular Helicity of Optically Active Poly(phenylacetylene)s Bearing Cyclodextrin Pendants Induced by Various External Stimuli. *J. Am. Chem. Soc.* **2006**, *128*, 7639–7650.

(23) Maeda, K.; Hirose, D.; Nozaki, M.; Shimizu, Y.; Mori, T.; Yamanaka, K.; Ogino, K.; Nishimura, T.; Taniguchi, T.; Moro, M.; Yashima, E. Helical Springs as a Color Indicator for Determining Chirality and Enantiomeric Excess. *Sci. Adv.* **2021**, *7*, eabg5381.

(24) Wang, S.; Xie, S.; Zeng, H.; Du, H.; Zhang, J.; Wan, X. Self-Reporting Activated Ester-Amine Reaction for Enantioselective Multi-Channel Visual Detection of Chiral Amines. *Angew. Chem., Int. Ed.* **2022**, DOI: 10.1002/anie.202202268.

(25) Yashima, E.; Maeda, K. Helical Polymers with Dynamic and Static Macromolecular Helicity Memory: The Power of Helicity Memory for Helical Polymer Synthesis and Applications. *Bull. Chem. Soc. Jpn.* **2021**, *94*, 2637–2661.

(26) Shimomura, K.; Ikai, T.; Kanoh, S.; Yashima, E.; Maeda, K. Switchable Enantioseparation Based on Macromolecular Memory of a Helical Polyacetylene in the Solid State. *Nat. Chem.* **2014**, *6*, 429–434.

(27) Ishidate, R.; Sato, T.; Ikai, T.; Kanoh, S.; Yashima, E.; Maeda, K. Helicity Induction and Memory Effect in Poly(biphenylylacetylene)s Bearing Various Functional Groups and Their Use as Switchable Chiral Stationary Phases for HPLC. *Polym. Chem.* **2019**, *10*, 6260–6268.

(28) Ikai, T.; Kurake, T.; Okuda, S.; Maeda, K.; Yashima, E. Racemic Monomer-Based One-Handed Helical Polymer Recognizes Enantiomers through Auto-Evolution of Its Helical Handedness Excess. *Angew. Chem., Int. Ed.* **2021**, *60*, 4625–4632.

(29) Ando, M.; Ishidate, R.; Ikai, T.; Maeda, K.; Yashima, E. Helicity Induction and Its Static Memory of Poly(biphenylylacetylene)s Bearing Pyridine *N*-Oxide Groups and Their Use as Asymmetric Organocatalysts. *J. Polym. Sci., Part A: Polym. Chem.* **2019**, *57*, 2481–2490.

(30) Ikai, T.; Okuda, S.; Yashima, E. Macromolecular Helicity Induction and Static Helicity Memory of Poly(biphenylylacetylene)s Bearing Aromatic Pendant Groups and Their Use as Chiral Stationary Phases for High-Performance Liquid Chromatography. *Chirality* **2022**, *34*, 306–316.

(31) Ikai, T.; Mizumoto, K.; Ishidate, R.; Kitzmann, W. R.; Ikeda, R.; Yokota, C.; Maeda, K.; Yashima, E. Catalytic One-Handed Helix-Induction and Memory of Amphiphilic Poly(biphenylylacetylene)s in Water. *Giant* **2020**, *2*, 100016.

(32) Maeda, K.; Hirose, D.; Okoshi, N.; Shimomura, K.; Wada, Y.; Ikai, T.; Kanoh, S.; Yashima, E. Direct Detection of Hardly Detectable Hidden Chirality of Hydrocarbons and Deuterated

Isotopomers by a Helical Polyacetylene through Chiral Amplification and Memory. *J. Am. Chem. Soc.* **2018**, *140*, 3270–3276.

(33) Ikai, T.; Takeda, S.; Yashima, E. Catalytic One-Handed Helix Induction and Subsequent Static Memory of Poly(biphenylylacetylene)s Assisted by a Small Amount of Carboxy Groups Introduced at the Pendants. *ACS Macro Lett.* **2022**, *11*, 525–531.

(34) Ikai, T.; Ando, M.; Ito, M.; Ishidate, R.; Suzuki, N.; Maeda, K.; Yashima, E. Emergence of Highly Enantioselective Catalytic Activity in a Helical Polymer Mediated by Deracemization of Racemic Pendants. *J. Am. Chem. Soc.* **2021**, *143*, 12725–12735.

(35) Ishidate, R.; Markvoort, A. J.; Maeda, K.; Yashima, E. Unexpectedly Strong Chiral Amplification of Chiral/Achiral and Chiral/Chiral Copolymers of Biphenylylacetylenes and Further Enhancement/Inversion and Memory of the Macromolecular Helicity. *J. Am. Chem. Soc.* **2019**, *141*, 7605–7614.

(36) Ikai, T.; Ishidate, R.; Inoue, K.; Kaygisiz, K.; Maeda, K.; Yashima, E. Chiral/Achiral Copolymers of Biphenylylacetylenes Bearing Various Substituents: Chiral Amplification through Copolymerization, Followed by Enhancement/Inversion and Memory of the Macromolecular Helicity. *Macromolecules* **2020**, *53*, 973–981.

(37) Simionescu, C. I.; Percec, V.; Dumitrescu, S. Polymerization of Acetylenic Derivatives. XXX. Isomers of Polyphenylacetylene. *J. Polym. Sci., Polym. Chem. Ed.* **1977**, *15*, 2497–2509.

(38) Simionescu, C. I.; Percec, V. Polypentadeuterophenylacetylene Isomers. *J. Polym. Sci., Polym. Chem. Ed.* **1979**, *17*, 421–429.

(39) Taniguchi, T.; Yoshida, T.; Echizen, K.; Takayama, K.; Nishimura, T.; Maeda, K. Facile and Versatile Synthesis of End-Functionalized Poly(phenylacetylene)s: A Multicomponent Catalytic System for Well-Controlled Living Polymerization of Phenylacetylenes. *Angew. Chem., Int. Ed.* **2020**, *59*, 8670–8680.

(40) The conventional rhodium-catalyzed polymerization of **2** with $[Rh(nbd)Cl]_2$ in THF/triethylamine afforded polymeric products, which were mostly insoluble in common organic solvents probably due to formation of extremely high molar-mass polymers.

(41) The helical sense of the PBPAs was tentatively assigned based on the analogous (*P*)- and (*M*)-handed helical poly(phenylacetylene)s showing similar CD spectra determined by direct observations of the helical structures by high-resolution atomic force microscopy, see, for example: ref 25. (a) Sakurai, S.; Okoshi, K.; Kumaki, J.; Yashima, E. Two-Dimensional Hierarchical Self-Assembly of One-Handed Helical Polymers on Graphite. *Angew. Chem., Int. Ed.* **2006**, *45*, 1245–1248. (b) Sakurai, S.; Okoshi, K.; Kumaki, J.; Yashima, E. Two-Dimensional Surface Chirality Control by Solvent-Induced Helicity Inversion of a Helical Polyacetylene on Graphite. *J. Am. Chem. Soc.* **2006**, *128*, 5650–5651. (c) Yashima, E. Synthesis and Structure Determination of Helical Polymers. *Polym. J.* **2010**, *42*, 3–16.

(42) The *hse* values were estimated using the maximum $\Delta\varepsilon_{2nd}$ value ($\Delta\varepsilon_{2nd}^{max} = 20$) of a fully one-handed helical PBPA composed of optically-pure monomer units at 25 °C, as the base value (see ref 35).

(43) Gao, G.; Sanda, F.; Masuda, T. Synthesis and Properties of Amino Acid-Based Polyacetylenes. *Macromolecules* **2003**, *36*, 3932–3937.

(44) Leiras, S.; Freire, F.; Seco, J. M.; Quiñoá, E.; Riguera, R. Controlled Modulation of the Helical Sense and the Elongation of Poly(phenylacetylene)s by Polar and Donor Effects. *Chem. Sci*. **2013**, *4*, 2735–2743.

(45) Sakai, R.; Satoh, T.; Kakuchi, T. Polyacetylenes as Colorimetric and Fluorescent Chemosensor for Anions. *Polym. Rev*. **2017**, *57*, 159–174.

(46) Zhou, Y.; Zhang, C.; Ma, R.; Liu, L. J.; Dong, H.; Satoh, T.; Okamoto, Y. Synthesis of Helical Poly(phenylacetylene) Derivatives Bearing Diastereomeric Pendants for Enantioseparation by HPLC. *New J. Chem*. **2019**, *43*, 3439–3446.

(47) For similar solvent-dependent CD and absorption spectral changes in the helical poly(phenylacetylene)s bearing L- or D-amino acid residues through amide (–NHCO–) linkers, see: (a) Maeda, K.; Kamiya, N.; Yashima, E. Poly(phenylacetylene)s Bearing a Peptide Pendant: Helical Conformational Changes of the Polymer Backbone Stimulated by the Pendant Conformational Change. *Chem. - Eur. J*. **2004**, *10*, 4000–4010. (b) Nishimura, T.; Maeda, K.; Ohsawa, S.; Yashima, E. Helical Arrays of Pendant Fullerenes on Optically Active Poly(phenylacetylene)s. *Chem. - Eur. J*. **2005**, *11*, 1181–1190. (c) Zhao, H. C.; Sanda, F.; Masuda, T. Synthesis and Chiroptical Properties of L-Serine-Based Poly(phenylacetylenes). *J. Macromol. Sci. Part A-Pure Appl. Chem*. **2007**, *44*, 389–394. (d) Suarez-Picado, E.; Quinoa, E.; Riguera, R.; Freire, F. Poly(phenylacetylene) Amines: A General Route to Water-Soluble Helical Polyamines. *Chem. Mater*. **2018**, *30*, 6908–6914. (e) Zhou, Y. L.; Zhang, C. H.; Zhou, Z. J.; Zhu, R. Q.; Liu, L. J.; Bai, J. W.; Dong, H. X.; Satoh, T.; Okamoto, Y. Influence of Different Sequences of L-Proline Dipeptide Derivatives in the Pendants on the Helix of Poly(Phenylacetylene)s and Their Enantioseparation Properties. *Polym. Chem*. **2019**, *10*, 4810–4817.

(48) Another seven-membered ring intrapendant H-bonding formation at each pendant of poly-**2**$^{\text{L-Leu}}$ could not be completely excluded. If this is the case, the steric repulsion between the bulky seven-membered ring pendants may cause such an extended-helix formation of poly-**2**$^{\text{L-Leu}}$ (Figures S10 and S11c).

(49) Tabata, M.; Tanaka, Y.; Sadahiro, Y.; Sone, T.; Yokota, K.; Miura, I. Pressure-Induced Cis to Trans Isomerization of Aromatic Polyacetylenes. 2. Poly((*o*-ethoxyphenyl)acetylene) Stereoregularly Polymerized Using a Rh Complex Catalyst. *Macromolecules* **1997**, *30*, 5200–5204.

(50) Tang, Z.; Iida, H.; Hu, H.-Y.; Yashima, E. Remarkable Enhancement of the Enantioselectivity of an Organocatalyzed Asymmetric Henry Reaction Assisted by Helical Poly(phenylacetylene)s Bearing Cinchona Alkaloid Pendants via an Amide Linkage. *ACS Macro Lett*. **2012**, *1*, 261–265.

(51) Maeda, K.; Maruta, M.; Shimomura, K.; Ikai, T.; Kanoh, S. Chiral Recognition Ability of an Optically Active Poly(diphenylacetylene) as a Chiral Stationary Phase for HPLC. *Chem. Lett*. **2016**, *45*, 1063–1065.

(52) Hirose, D.; Nozaki, M.; Maruta, M.; Maeda, K. Solvent-Dependent Helix Inversion in Optically Active Poly(diphenylacetylene)s and Their Chiral Recognition Abilities as Chiral Stationary Phases for High-Performance Liquid Chromatography. *Chirality* **2022**, *34*, 597–608.

(53) Hirose, D.; Isobe, A.; Quiñoá, E.; Freire, F.; Maeda, K. Three-State Switchable Chiral Stationary Phase Based on Helicity Control of an Optically Active Poly(phenylacetylene) Derivative by Using Metal Cations in the Solid State. *J. Am. Chem. Soc*. **2019**, *141*, 8592–8598.

(54) For helical polymer-based switchable CSPs upon thermal annealing[51,52] or by the addition of metal cations[53] showing reversed elution orders of the enantiomers, see refs 51–53.

TOC

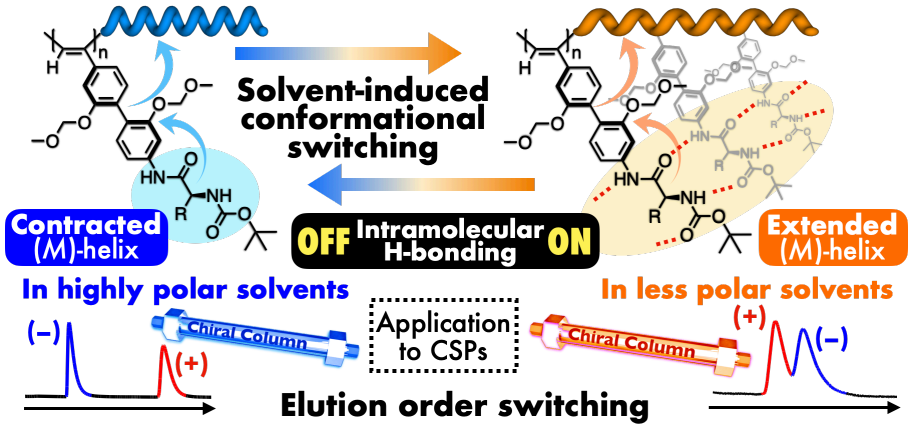
Solvent-induced conformational switching
Contracted (M)-helix
OFF Intramolecular H-bonding ON
Extended (M)-helix
In highly polar solvents
In less polar solvents
Chiral Column
Application to CSPs
Chiral Column
(–)
(+)
(+)
(–)
Elution order switching